東海大學

資訊工程研究所

碩士論文

指導教授：黃育仁 教授

Advisor：Associate Professor Yu-Len Huang

基於 Level-set 方法的 3D 超音波乳房腫瘤切割

Breast tumor segmentation based on level-set method in 3D sonography

研究生：林昱志

Name：Yu-Chih Lin

中 華 民 國 一 0 二 年 七 月

July 2013

Breast tumor segmentation based on level-set method in 3D sonography

Advisor

Prof. Yu-Len Huang

Department of Computer Science

Tunghai University

Submitted in Partial Fulfillment

of the Requirements for the Degree

Master of Engineering

by

Yu-Chih Lin

July 2013

東海大學碩士學位論文考試審定書

東海大學資訊工程學系 研究所

研究生 林 昱 志 所提之論文

基於 Level-set 方法的 3D 超音波乳房腫瘤切割

經本委員會審查，符合碩士學位論文標準。

學位考試委員會
召 集 人 沈偉誌 簽章

委 員 康立威

黃育仁

指 導 教 授 黃育仁 簽章

中華民國 102 年 6 月 18 日

摘要

在超音波影像中，良性和惡性乳房腫瘤的形狀和大小有顯著的差異。然而，超音波影像經常包含大量的雜訊及紋理特徵，診斷時必需高度依賴醫生的專業知識與臨床經驗，所以提供腫瘤輪廓的型態資訊在臨床診斷上是非常重要的。手動方式繪製三維(3D)乳房腫瘤輪廓是一個耗時而複雜的工作，自動化的超音波乳房腫瘤輪廓描繪可提供一個類似於手動描繪的成果，這將有助於醫生作出準確的診斷，提升醫師診斷腫瘤良惡性的正確率。本研究提出了一種基於等位函數集(level-set)方法的自動化三維超音波乳房腫瘤輪廓的檢測程序，此方法得到了類似手動描繪的乳房腫瘤輪廓，並且節省繪製精確的輪廓所需的大量時間。

關鍵字：乳癌、超音波影像、影像切割、三維區域成長法、腫瘤輪廓切割

ABSTRACT

Malignant and benign breast tumor present differently in their shape and size on sonography. Morphological information provided by the contour of tumor is important in clinical diagnosis. However, ultrasound images contain noises and tissue texture; clinical diagnosis thus highly depends on the experience of physicians. The manual way to sketch three-dimensional (3D) breast tumor contours is a time-consuming and complicated task. Automatic contouring provided the similar breast tumor contour by manual sketch in the ultrasonic images, that might assist physicians in making an accurate diagnosis. This study presents an efficient segmentation procedure based on level-set method for detecting contours of breast tumors automatically in 3D sonography. The proposed method suggested similar contours as if they were obtained by manually contouring for the breast tumor and could save much of the time required to sketch precise contours.

Keywords: breast cancer, 3D sonography, image segmentation, level-set method, region growing

INDEX

LIST OF TABLES

LIST OF FIGURES

CHAPTER1

INTRODUCTION

Ultrasound system can provide real-time images without radiation, and breast cancer examination using three-dimensional (3D) sonogram is gradually accepted by most people currently. Breast cancer is a tumor emerged from growing mammary epithelial cells or lobular, they lost control because of the growth of cancer cells and then will invade and damage nearby tissues and organs or metastasis to other organs through the blood or lymphatic system. However, breast is rich in blood vessels, lymphatic vessels and lymph nodes, so breast cancer cells tend to spread to other organs easily.

Breast cancer is one of the most frequently occurring cancers in women. According to the American Cancer Society (ACS) statistics, the prevalence of breast cancer rises up every year [1]. In 2013, about 232,340 American women were diagnosed with breast cancer, there increase 17.2% compared with 2009's 192,370. But as medical technology progress continuously and personal health concerns increase constantly, making the breast cancer death rate decreased year by year. In 2013, women's deaths due to breast cancer in USA were 39,620 people, a decrease of 1.37% of than 40,170 in 2009. Early detection and early treatment for breast cancer would reduce breast cancer mortality.

Due to ultrasound equipment has a low-cost, convenience, and other advantages, ultrasound becomes the essential diagnostic tools for hospitals of any size. Physicians also assisted by computer-aided diagnosis (CAD) system [2] to retrieve useful information as a basis for diagnosis. Recently, 3D ultrasound images of the breast cancer screening have gradually gained attention. 3D ultrasound provides similar imaging quality to conventional two-dimensional (2D) ultrasound and also has the multi-sectional capability to reveal anatomical features what are not originally possible on a 2D system.

Physician could employ CAD as a second opinion to detect the characteristics of the tumor ultrasound image, which is helpful on the diagnosis. However, textural feature is not easy to do judgment by visual due to it is mostly unapparent in the 3D breast ultrasound image. To use image processing techniques to observe subtle changes in the image and by the help of CAD is particularly important.

The accuracy of CAD is related to the location and extent of tumor, the segmentation of the tumor has a direct impact on the accuracy of medical diagnosis. Contour of breast tumor can be sketched in manual, semi-automatic, or fully automatic manner [3-6]. However, the manual segmentation method is not suitable for 3D sonogram. A 3D sonogram in one scan can take over hundreds of 2D image slices, which require a lot of time for physician to complete all segmentation manually.

Although it can be extremely helpful if segmentation can be done automatically, automated segmentation techniques of breast cancer on 3D sonogram are still a very difficult problem [7]. Ultrasound images had a lot of spots, noise, shadow and tissue texture; in addition, compared with the benign tumors, the edge of malignant tumors seemed more irregular, crushing and splitting, leading to the automatic segmentation execution becomes more difficult. Most of segmentation methods for 3D ultrasound images still utilized semi-automatic way to make up for technical shortcomings. The operations of complexity and efficiency, the stable results of the execution are also worth consideration factors.

In computer vision, image segmentation is the process of partitioning a digital image into multiple segments. The purpose of image segmentation is to simplify or change the representation of the image, making the image easier to understand and analyze [8]. Image segmentation is typically used to locate objects and boundaries (lines, curves, etc.) in images. More precisely, image segmentation is the process of assigning a label to every pixel in an image such that pixels with the same label share certain visual characteristics. There have been many notable works on the image cutting methods, such as watershed transformation, K-means algorithm, region-based segmentation and active contour model algorithms.

The watershed transform [9-11] exercises the concept of topography and treats

digital image as a topographic plane. The pixel with highest value is the highest point on the terrain, the larger the change of the values indicates a more steeper terrain. However, this region-based segmentation method is very sensitive to noise, and had the over-segmentation problem [12]. Preprocessing with noise suppression is thus considered necessary for watershed transform to obtain a better result.

K-means clustering [13-14] segmented image into K clusters iteratively, mainly inside the large amounts of data to find the most representative data points. The so-called data points which can be called cluster centers and are classified according to the cluster center. The data is divided into many clusters through repeated iteration until no changes and then the method can create the effect of clustering segmentation. However, the K-means clustering data is also sensitive to noise and isolated points. This method must set the number of clusters, and excessive dependence on the initial value.

On the other hand, region-based segmentation according to the similarity of pixels, gathered the pixels into one area by exploiting the grayscale brightness, color and material. Equivalent to the whole image is divided into a block. However, the disadvantage of this method is too dependent on the characteristics of the image. The active contour model algorithm [15] proposed by Kass and Witkin, also known as snake algorithm, mainly used in two-dimensional image analysis and machine vision

image boundary detection, the purpose is to find the object boundary. Although active contour can be more accurately search the boundary of the object, the drawback is the need to enter the starting boundary and works on single target only.

Summary of the above-mentioned advantages and disadvantages, 3D images has more detailed structural information, researchers can gain more detail the characteristics, physician also has more reference for diagnosis. This study designed a 3D ultrasound images segmentation method to combine region growing and improved active contour algorithm – the level-set method.

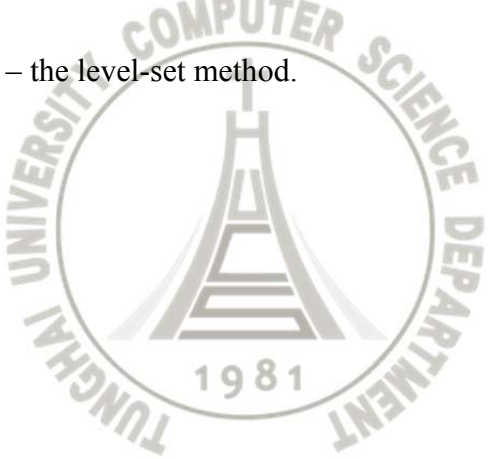

CHAPTER2

MATERIALS AND METHODS

The quality of initial contour not only influences to the final segmentation result, but also has a close relationship with the computation time required performing segmentation. Therefore the proposed method first utilized the 6-neighbors 3D region growing method to generate the initial contour. Then the closing algorithm [16] was used to process the data generated by 3D region growing. The purpose of closing algorithm method is to interrupt part again on link up with, and elimination of small holes, cracks, and elongated pit; and then fill the gap on the contour to smooth the edge. Finally, combined the initial contour and level-set algorithm, this study will get the desired segmentation results. Figure 1 shows the flowchart of the proposed method.

2.1 INITIAL CONTOUR

The seeded region growing algorithm [17-18] was to select a pixel as the core to grow. To determine that the seed surrounding pixels whether to have similar characteristics with the seed pixel, like gray-scale values, joints and colors. If the surrounding pixels had similar characteristics with the seed pixel, the surrounding pixel was accepted into the same region and then used as the new core. This process

continued on every surrounding pixel not classified until all pixels of the image were classified. When neighboring pixel and seed pixel gap was less than a threshold value, then the pixel vested in this area, the evolution gone until the region can't grow outside and formulate a closed area.

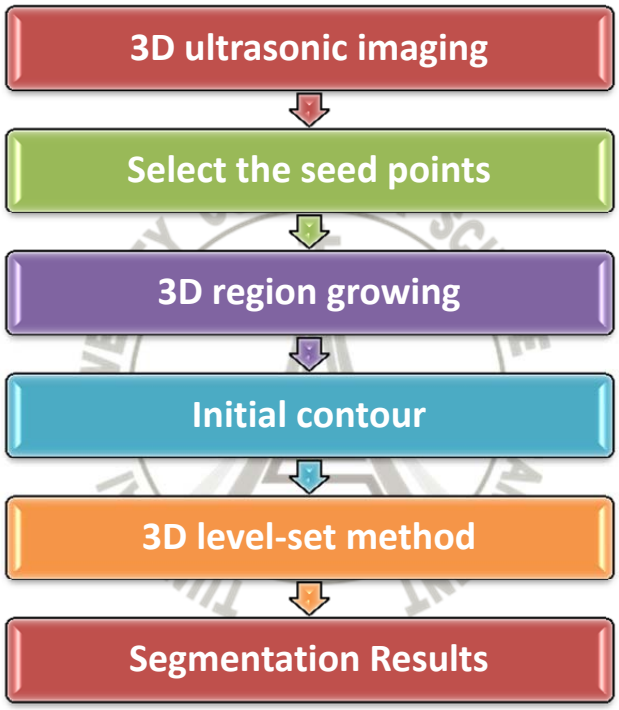

Figure 1. Flowchart of the proposed method

This study extracted the initial contour by using the 3D region growing method [19]. The first step was to circle the slice of maximum tumor extent and manually selected the seed points by doctor. The initial seed point for 3D regional growth was utilized by six neighbors [20-21] (6-connectivity) along the seed point: front, rear, left, right, upper and lower direction, to find a similar part with the pixels image intensity

values (see Fig.2), and then the procedure repeated to stop the expansion. The 6-neighboring method is faster than the traditional 26-neighboring method. The 3D level-set method required a great amount of computation and need to rely on the initial contour of set, thus this work utilized the 3D region growing method to generate the initial contour.

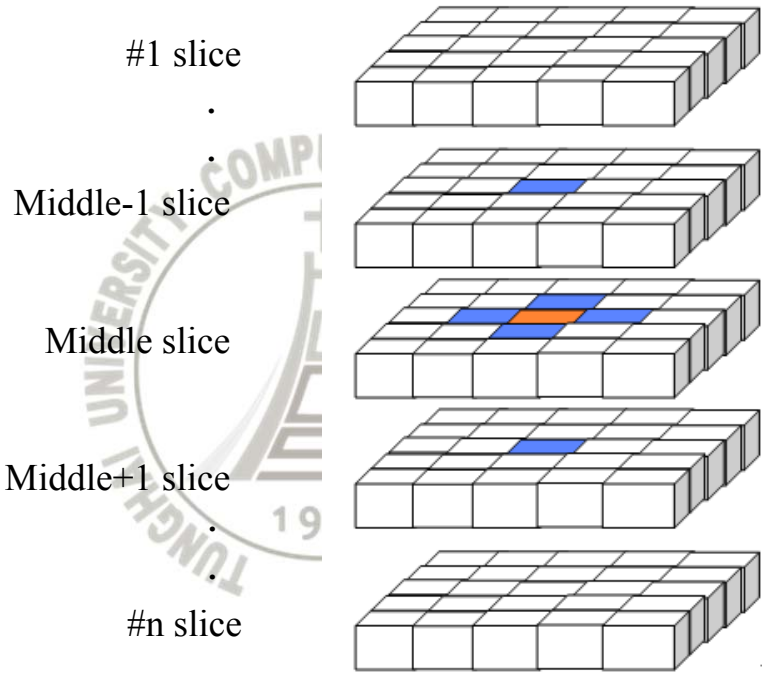

Figure 2. Neighbors (the blue voxels) within the 6-connectivity

This study used the seed point selected by the physician as a starting point for region growing. The seed point belongs to the tumor region is set to *A* and the threshold value is *T*. If any of the adjacent voxels and the seed point had a difference less than the threshold *T*, the proposed method put the adjacent voxel incorporated into the same region with the seed point and re-calculated the average pixel value of

the area *A*. Then the new incorporated pixel was used as a new starting point, looking for its six adjacent voxels, repeating the above steps until stopped the expansion.

$$T_d(V(x),A)=|V(x)-Am(V(x))|, \quad (1)$$

where $T_d(V(x),A)$ represents the absolute difference value between voxel *V(x)* and average pixel value in the area *A*. *V(x)* represents one of the six neighboring voxels. *Am(V(x))* represents the average value of the six neighbors.

$$\begin{cases} A=A \cup V(x) & \text{if } T_d(x,A)<T \\ A=A & \text{if } T_d(x,A)>T \end{cases}. \quad (2)$$

When the difference between the average voxel value of the voxel *V(x)* and the area *A* value was less than the threshold value *T* indicates that the voxel to be similar with pixel area *A*. The probability of belonging to the same tumor area was relatively large, this study utilized the voxel to merge into the same area; when the difference between the average voxel value of the voxel *V(x)* and the area *A* value was greater than the threshold value *T*, the probability of belonging to the same tumor area was relatively smaller, thus the proposed method rejected the voxel to merge into the same area.

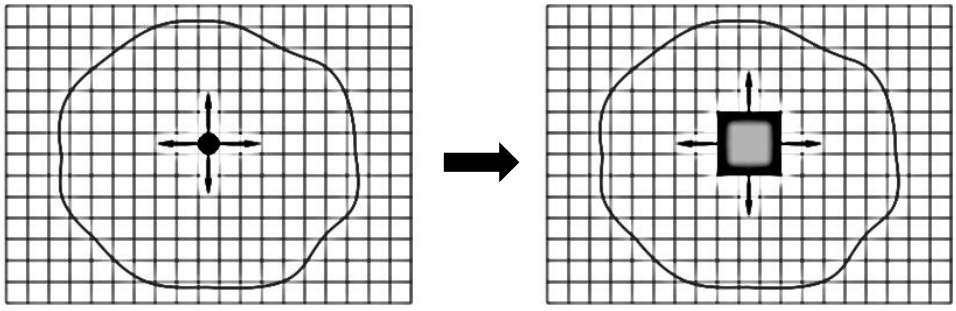

● Seed Pixel ↑ Direction Growth ■Grown Pixels ○ Pixels Being Considered

Figure 3. Illustrations of the seeded region growing

2.2 IMAGE SEGMENTATION

The basic idea of the level-set method [22-23] is that the plane closed curve expressed as a 3D continuous function surfaces having the same function value curve $\varphi(x, y)$ is usually $\varphi = 0$, known as the zero level-set, and the $\varphi(x, y)$ is also called level-set function. The level-set method is a way to denote active contours [24]. The zero level-set contour of the function is defined by

$$C\ \{(x, y)|\varphi(x, y)= 0\}. \tag{3}$$

Moreover, the inside region and the outside region of the curve are defined as:

$$\begin{cases} \varphi(x, y)>0 & \text{outside region} \\ \varphi(x, y)=0 & \text{contour} \\ \varphi(x, y)<0 & \text{inside region} \end{cases} . \tag{4}$$

In the level-set method, $\varphi = 0$ represents the contour that we want, $\varphi < 0$ is the internal region of the contour, and $\varphi > 0$ is the external region of the contour, so we

can absolutely depending on the value of the function to define the outline of its internal and external, as shown in Figure 4.

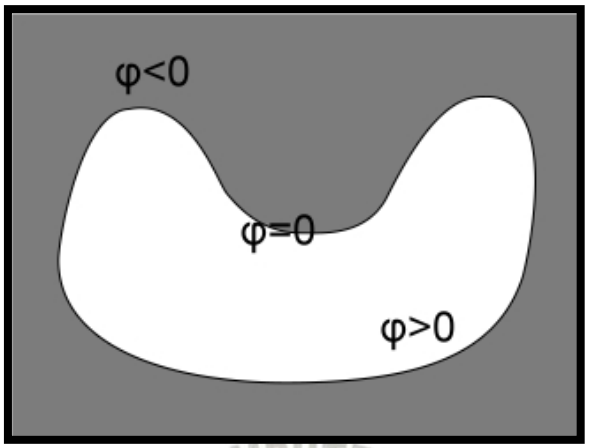

Figure 4. Illustrations of the level-set method

Take a closed curve as a boundary, the entire plane is divided into two areas: the external and internal regions of the curve. In the plane defined distance function $\varphi(x, y, t) = \pm d$, where d is the point (x, y) to the shortest distance of the curve, function symbols depending on the point in the curve of the internal or external, generally defined curve interior points the distance is negative, t represents time. At any moment, the point on the curve is the zero point of distance function value, i.e. a function of distance to the zero level set. Level-set method not only can handle a sharp endpoint and concave angle, but also can be automated to change the topology. There are two main advantages to represent the active contour by level set method. First, it can easily represent complicated contour changes, for example when the contour splits into two or develops holes inside. Second, we can easily know whether

a point is inside or outside the contour by checking its φ value.

This study used Chen-Vese method, where φ is updated as

$$\Delta\varphi=\delta(\varphi)\left\{\mu\cdot\mathrm{div}\left(\frac{\nabla\varphi}{|\nabla\varphi|}\right)-\lambda_1(u_0-c_1)^2+\lambda_2(u_0-c_2)^2-v\right\}, \quad (5)$$

where u_0 is the original image, *c1* and *c2* are the average gray level intensity in $\varphi>0$ region and $\varphi<0$ region, respectively. Moreover, φ is the level set function, μ 、λ_1 、λ_2 、v are parameters which adjust the weights of the four terms and δ is the Dirac delta function which used to make the contour smooth and can eliminate some small isolated regions, i.e. noises. The second and the third terms are the driving force term which drives contour to move towards the equilibrium point of the gray level values of the internal and external.

The proposed method can see that the contour evolution is based on gray-scale value of the internal and external contours, it do not use any gradient information. Therefore this method can work under condition that the edge is not very apparent. The results of the 3D region growing were performed as an initial contour and then the 3D level-set procedure was used to obtain the final segmentation results.

2.3 DATA ACQUISITION

There collected 10 benign and 10 malignant breast tumor patients aged from 17

to 80 years old (mean age 44 years). About 120 to 280 ultrasound images of each case, and the average image size of 183×108 pixels. In this study, sonographic examinations were done by using 3D power Doppler ultrasound with the high definition flow (HDF) function (Voluson 730, GE Medical Systems, Zipf, Austria). A linear-array broadband probe with a frequency of 6–12 MHz, a scan width of 37.5 mm, and a sweep angle of 5◦ to 29◦ to obtain 3D volume scanning was used. Physician kept a fixed sweep angle of 20◦ and power Doppler settings of mid frequency, 0.9 kHz pulse repetition frequency, -0.6 gain, and 'low 1' wall motion filter in all cases. All obtained images were stored on the hard disk and transferred to a personal computer using a DICOM (Digital Imaging and Communications in Medicine) connection for image analysis.

2.4 MANUAL CONTOURING

An experienced physician who was familiar with breast ultrasound interpretations manually determined 3D contours of the tumor by using two distinct modes. The entire manual sketching (EMS) mode denoted physician manually sketched 2D contour on each slice of a tumor. The partial manual sketching mode denoted the virtual organ computer-aided analysis (VOCAL) [25-27] scheme within 4D View software (GE Medical Systems, Zipf, Austria) was performed to obtain an

approximated 3D contour. Then the obtained contours were saved in files for comparison with the automatically generated contours. The VOCAL scheme estimates 3D contours by a selectable degree of rotation. This study adopted a very common rotation degree 30^{o}, the six preliminary tumor contours in 0°, 30°, 60°, 90°, 120° and 150° slice images were manually sketched. Figure 5 represents the tumor contour manually sketched with 30° rotation. The VOCAL mode utilized the six extracted tumor regions to build a 3D interested region volume.

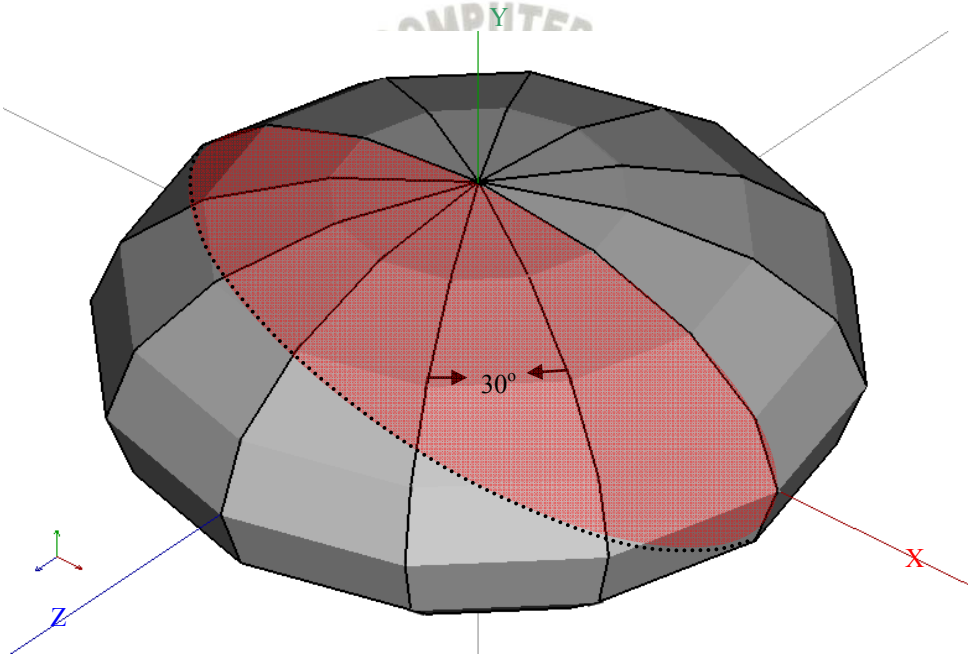

Figure 5. The tumor contour that manually sketched with 30◦ by export

2.5 EVALUATION OF CONTOUR

The four practical similarity measures [28], the similarity index (SI), overlap value (OV), overlap fraction (OF) and extra fraction (EF) between the manually determined contours and the automatically detected contours were calculated for quantitative analysis of the contouring results. REF represents the results depicted by the physician manually, and SEG indicates our proposed segmentation method. The relationship between SEG and REF, overlap area denotes the area covered by proposed segmentation algorithm and manual sketching by physician, extra area denotes the false positive area and missing area denotes false negatives area.

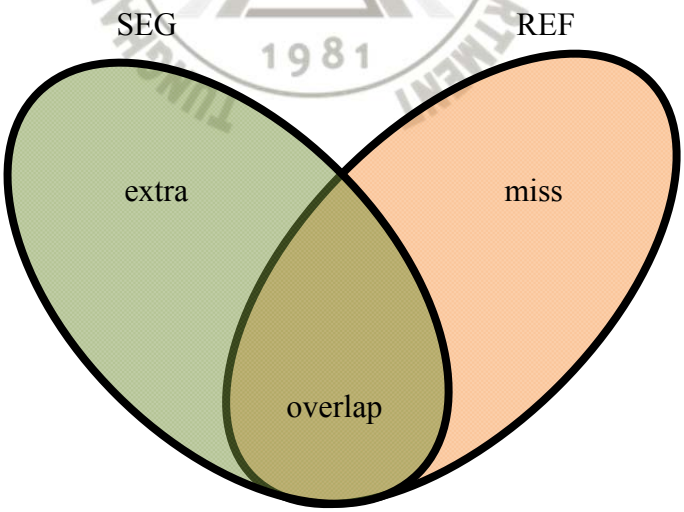

Figure 6. Schematic diagram evaluation of contour

Figure 6 illustrates the relationship between the SEG and REF. When SI, OV and OF are close to 1, and EF computation is close to 0, it means that the contours

generated by automatic segmentation is similar to the manual contours by physician. The overlap denotes the area of the intersection of the reference and the automated segmentation. The SI expresses the similar degree between SEG and REF areas. The SI, OF, OV and EF are defined:

$$SI = \frac{2\times(REF\cap SEG)}{REF+SEG} \times 100\% \ , \tag{5}$$

$$OF = \frac{REF\cap SEG}{REF} \times 100\% \ , \tag{6}$$

$$OV = \frac{REF\cap SEG}{REF\cup SEG} \times 100\% \ , \tag{7}$$

$$EF = \frac{REF\cap SEG}{REF} \times 100\% \ . \tag{8}$$

CHAPTER3

EXPERIMENTAL RESULT

This study utilized the similarity measures to evaluate the tumor contours generated by the proposed segmentation method and the virtual organ computer-aided analysis (VOCAL) with 30^{o} rotations. The simulations totally evaluated 20 cases with manual sketched contours (including 10 benign breast tumors and 10 malignant ones) to test the accuracy of the proposed contouring method. The simulations were made on a single CPU Intel(R) Core(TM) i5-2400 3.10GHz personal computer with Microsoft Windows 7 professional operating system and the program development environment was MATLAB (R2011.a) software (The MathWorks, Inc., Natick, MA).

In this study, the region growing threshold T was initially set to 5, its value will be automatically adjusted due to the implementation of the frequency and time; closing algorithm mask size was set to 20×20. Before the execution of the level-set algorithm, the first step performed the 3D Gaussian blur pretreatment of the breast tumor, sigma of value was 1.5, the mask is 3×3 matrix. Finally, this study executed 2 cycles in level-set algorithm. Weight for the smooth term is 1, weight for the image term is 1×10^{-6}, time step for each iteration was 1.

Table 1 shows contouring performance of the proposed method, and Table 2

shows contouring performance of the VOCAL method. The average of the measures (SI, OV, OF, EF) that determined by the proposed method and the VOCAL method were (0.85, 0.84, 0.75, 0.13) and (0.81, 0.92, 0.69, 0.34). Figures 7 shows the automatic sketched contours (in 2D view) obtained by using the proposed method. Average execution time for each case was 60 seconds. As this scheme is an offline diagnostic application, these segmentation times are clinically acceptable.

Figure 8(a) is the contour of a benign tumor that drawn manually by a doctor. Figure 8(b) is the result of obtained benign tumor contour segmentation by our proposed LSM method. Figure 8(c) is a benign tumor contour result obtained by using the VOCAL method. Figure 9(a) is the contour of a malignant tumor that drawn manually by a doctor. Figure 9(b) is the result of obtained malignant tumor contour segmentation by our proposed LSM method. Figure 9(c) is a malignant tumor contour result obtained by using the VOCAL method.

Figures 10 to 13 show the results of the assessment of the proposed LSM method and the VOCAL method. We can be seen from Figures 8 to 13, compared to our proposed the LSM tumor contour segmentation method and VOCAL method, it not only more accurate segmentation results, but also significantly shorten the operation time of the program.

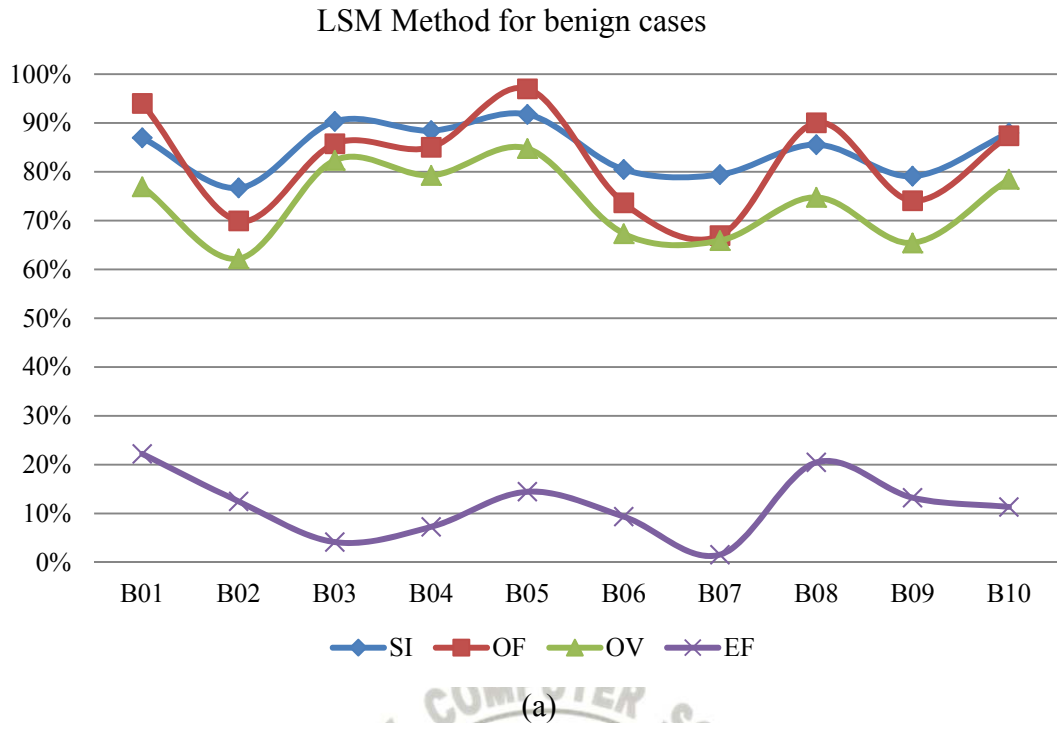

(a)

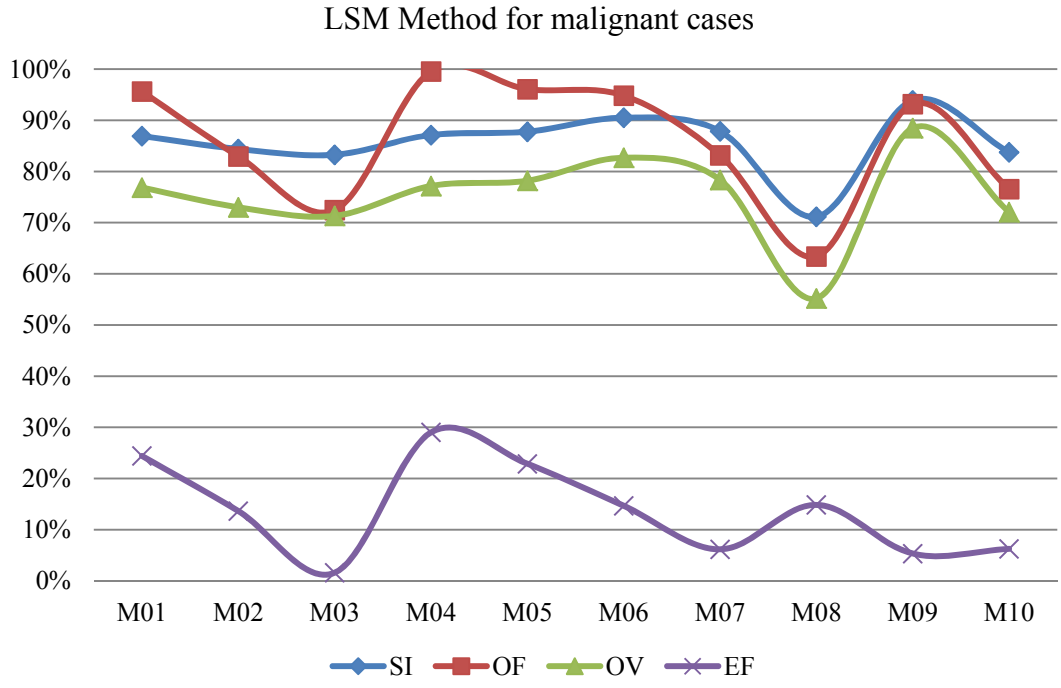

(b)

Figure 7. Evaluation of segmentation results: (a) benign cases; (b) malignant cases. SI: similarity index; OF: overlap fraction; OV: overlap value; EF: extra fraction

Table 1. The proposed method utilized 3D level-set results of the evaluation

Case	SI	OF	OV	EF
B01	86.97%	94.04%	76.95%	22.22%
B02	76.70%	69.96%	62.20%	12.47%
B03	90.33%	85.77%	82.36%	4.14%
B04	88.44%	85.03%	79.28%	7.26%
B05	91.76%	97.02%	84.77%	14.46%
B06	80.48%	73.65%	67.33%	9.37%
B07	79.45%	66.94%	65.91%	1.56%
B08	85.56%	90.06%	74.77%	20.46%
B09	79.11%	74.09%	65.44%	13.23%
B10	87.95%	87.39%	78.49%	11.34%
M01	86.92%	95.64%	76.86%	24.42%
M02	84.39%	82.96%	73.00%	13.64%
M03	83.27%	72.46%	71.33%	1.58%
M04	87.12%	99.56%	77.17%	29.01%
M05	87.77%	96.08%	78.20%	22.87%
M06	90.52%	94.82%	82.69%	14.67%
M07	87.87%	83.18%	78.36%	6.15%
M08	71.14%	63.40%	55.20%	14.85%
M09	93.88%	93.18%	88.47%	5.32%
M10	83.77%	76.58%	72.07%	6.25%
Average	**85.17%**	**84.09%**	**74.54%**	**12.76%**

Table 2. The VOCAL method results of the evaluation

Case	SI	OF	OV	EF
B01	83.43%	96.57%	71.56%	34.94%
B02	64.56%	64.13%	47.67%	34.52%
B03	86.67%	92.14%	76.47%	20.48%
B04	85.44%	92.96%	74.57%	24.66%
B05	83.39%	95.06%	71.51%	32.94%
B06	88.23%	97.59%	78.95%	23.62%
B07	84.22%	92.40%	72.74%	27.02%
B08	82.32%	88.75%	69.95%	26.87%
B09	70.56%	63.64%	54.51%	16.75%
B10	79.24%	93.34%	65.62%	42.25%
M01	73.73%	97.93%	58.39%	67.71%
M02	80.97%	95.93%	68.03%	41.02%
M03	82.62%	96.50%	70.38%	37.11%
M04	84.13%	96.03%	72.61%	32.25%
M05	83.77%	95.35%	72.07%	32.30%
M06	83.29%	96.93%	71.36%	35.84%
M07	83.85%	94.21%	72.19%	30.50%
M08	79.84%	91.77%	66.45%	38.10%
M09	84.15%	99.09%	72.64%	36.42%
M10	82.76%	97.07%	70.59%	37.51%
Average	**81.36%**	**91.87%**	**68.91%**	**33.64%**

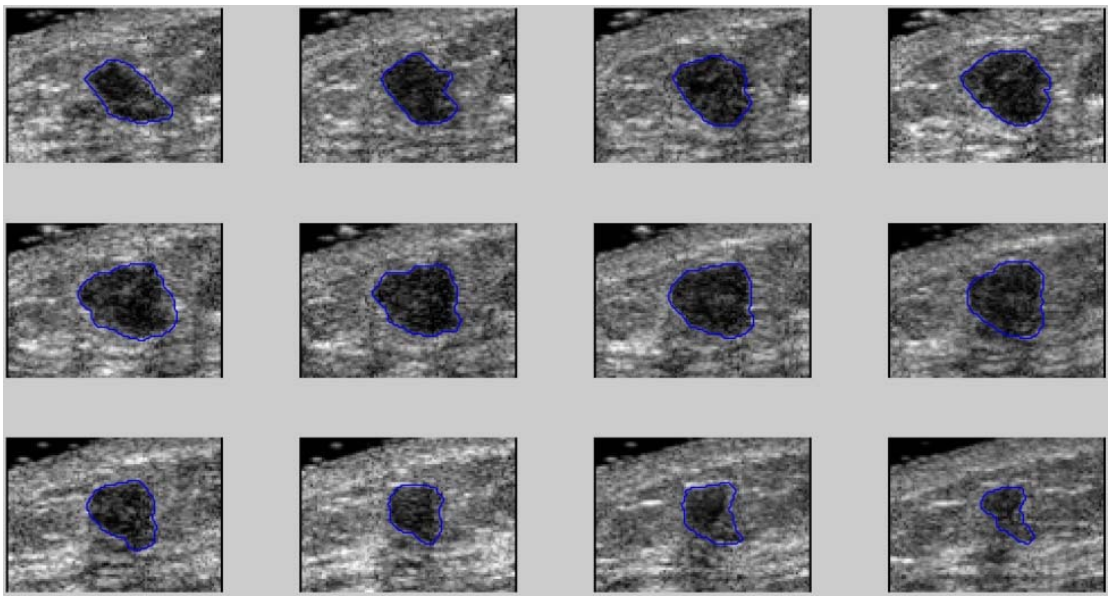

(a)

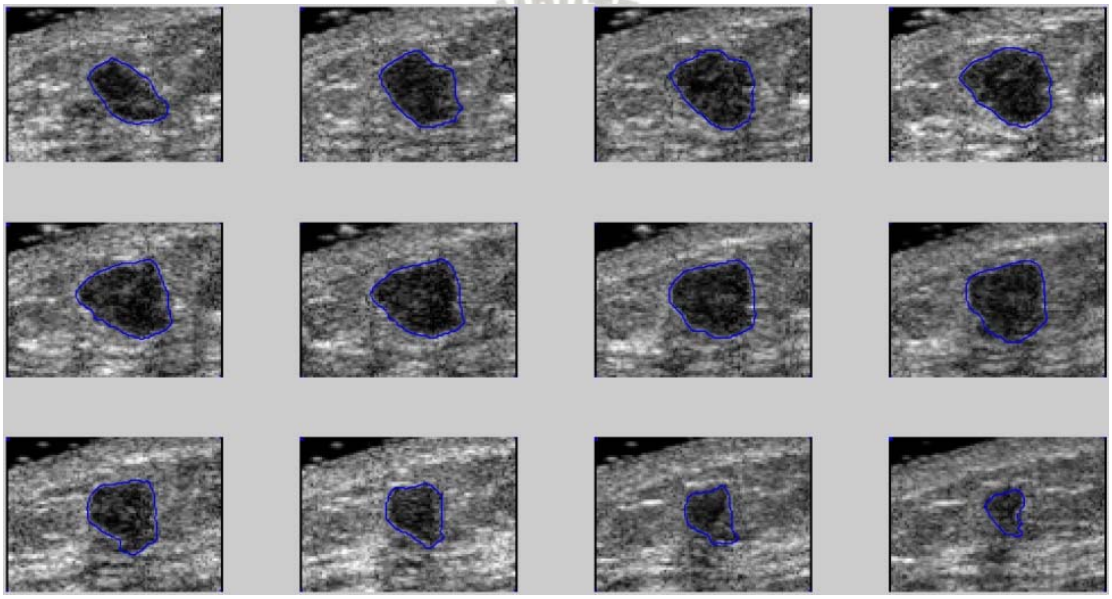

(b)

Figure 8. Results of contour segmentation with benign case: (a) is the benign tumor contour that drawn manually by a doctor; (b) is the result of obtained benign tumor contour segmentation by our proposed LSM method; (c) is a benign tumor contour results obtained by using the VOCAL method (continued)

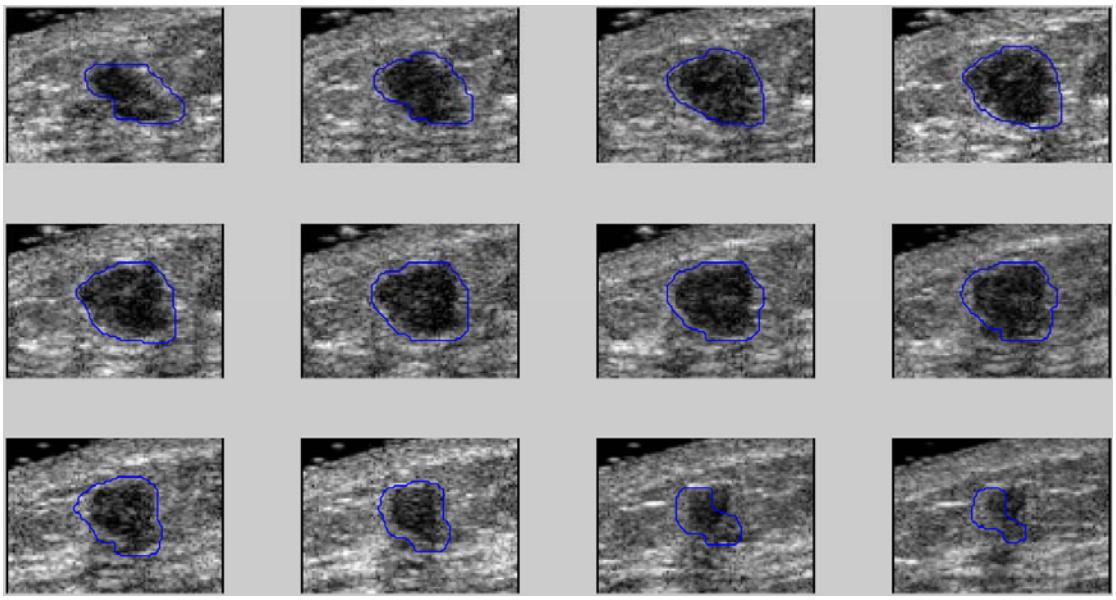

(c)

Figure 9. Results of contour segmentation with benign case: (a) is the benign tumor contour that drawn manually by a doctor; (b) is the result of obtained benign tumor contour segmentation by our proposed LSM method; (c) is a benign tumor contour results obtained by using the VOCAL method

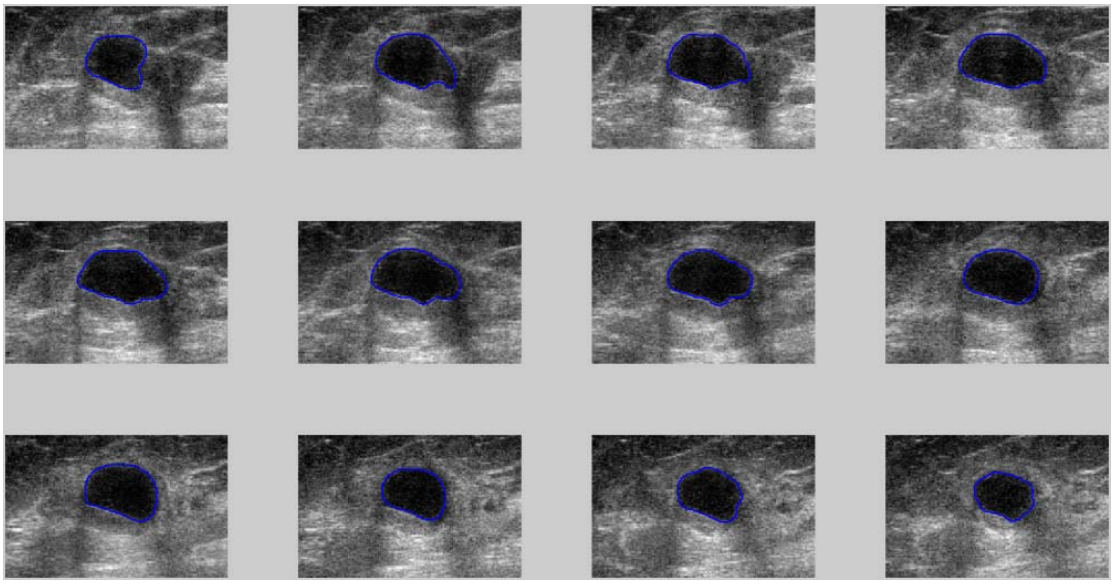

(a)

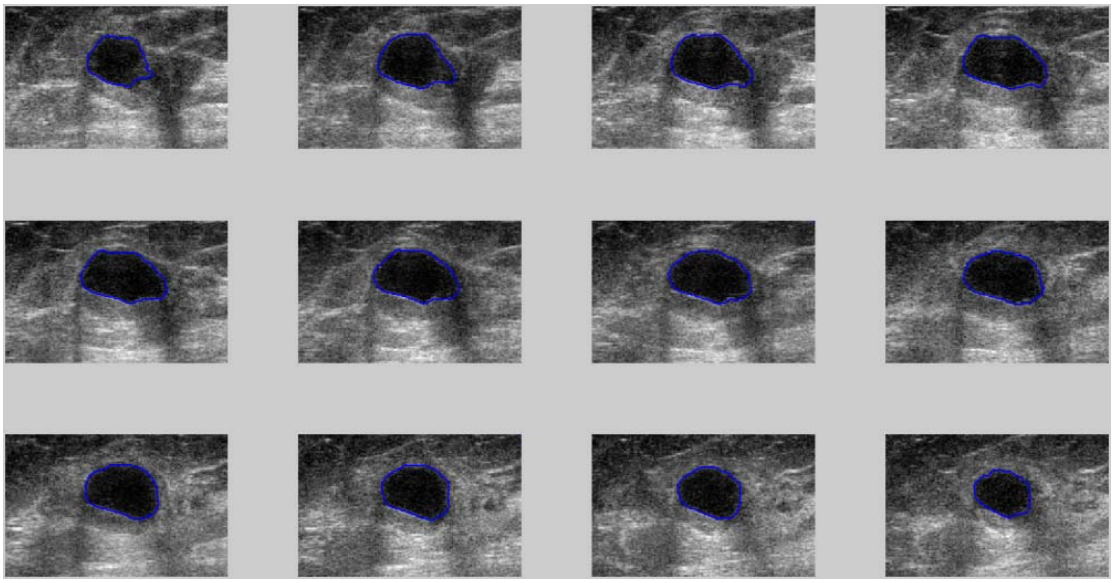

(b)

Figure 10. Results of contour segmentation with malignant case: (a) is the malignant tumor contour that drawn manually by a doctor; (b) is the result of obtained malignant tumor contour segmentation by our proposed LSM method; (c) is a malignant tumor contour results obtained by using the VOCAL method (continued)

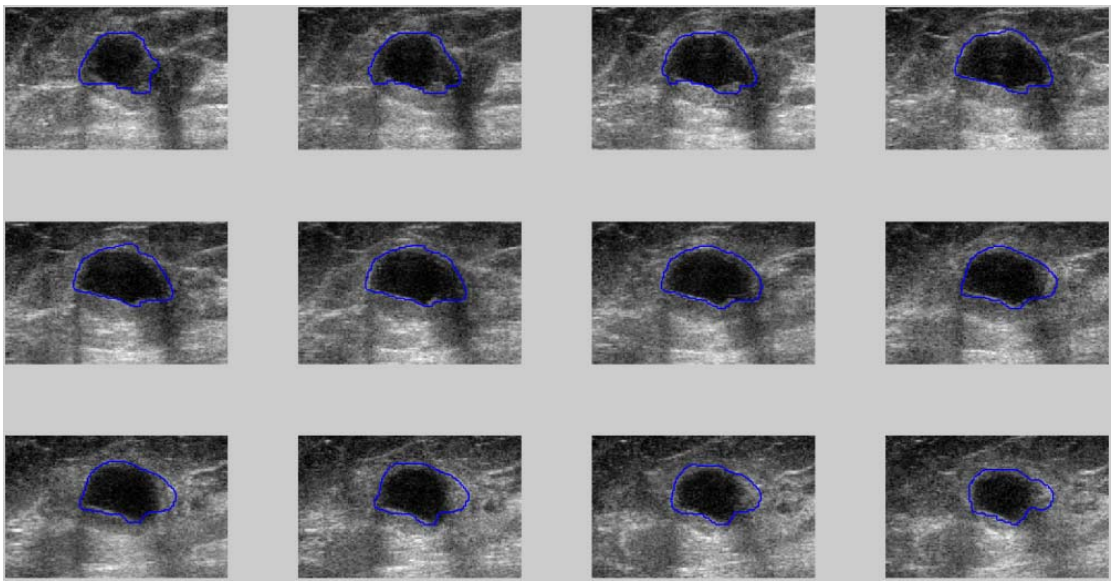

(c)

Figure 11. Results of contour segmentation with malignant case: (a) is the malignant tumor contour that drawn manually by a doctor; (b) is the result of obtained malignant tumor contour segmentation by our proposed LSM method; (c) is a malignant tumor contour results obtained by using the VOCAL method

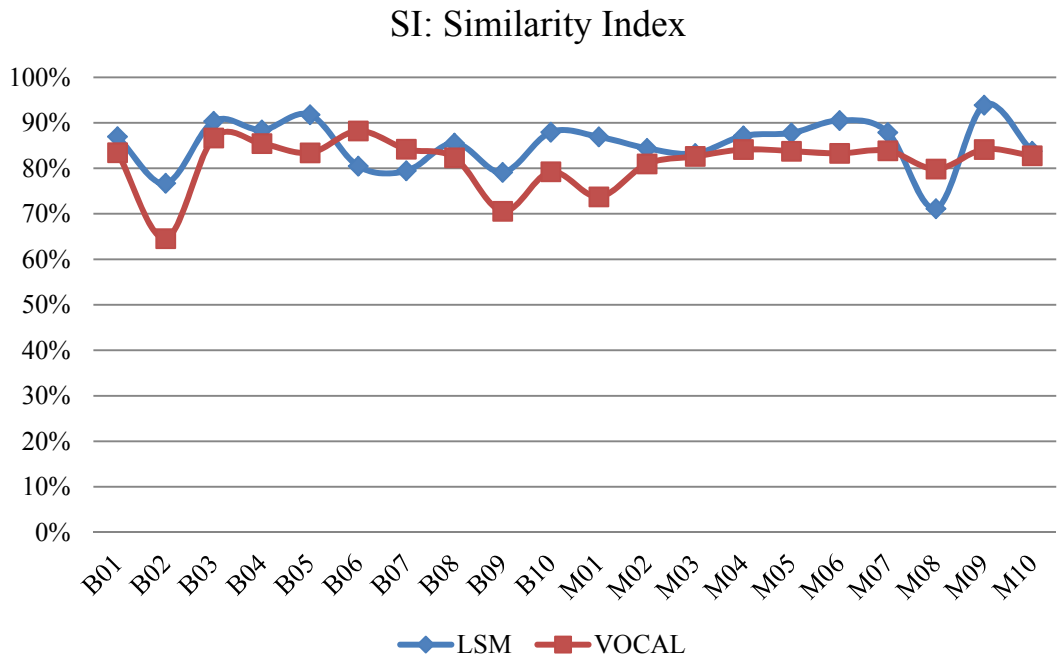

Figure 12. The similarity index (SI) evaluation results of the assessment of our proposed LSM method and the VOCAL method

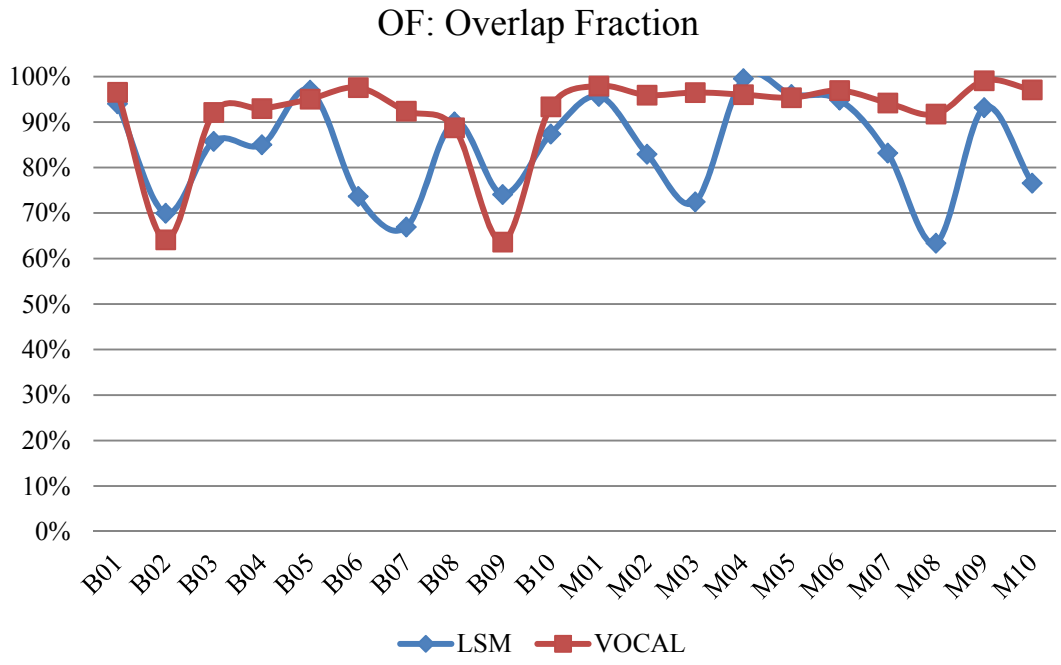

Figure 13. The overlap fraction (OF) evaluation results of the assessment of our proposed LSM method and the VOCAL method

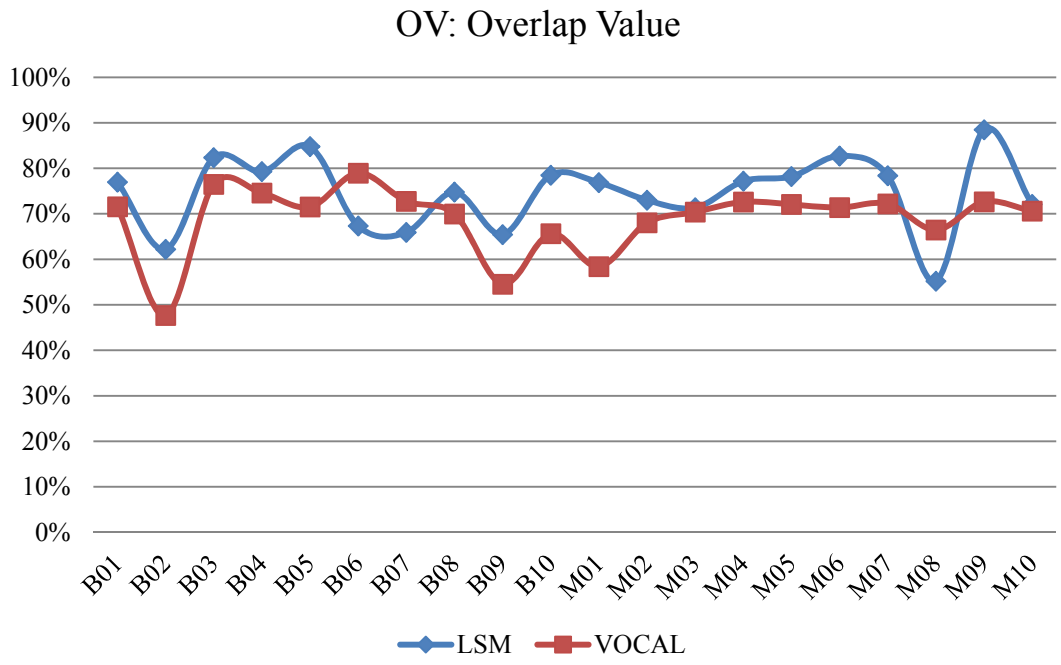

Figure 14. The overlap value (OV) evaluation results of the assessment of our proposed LSM method and the VOCAL method

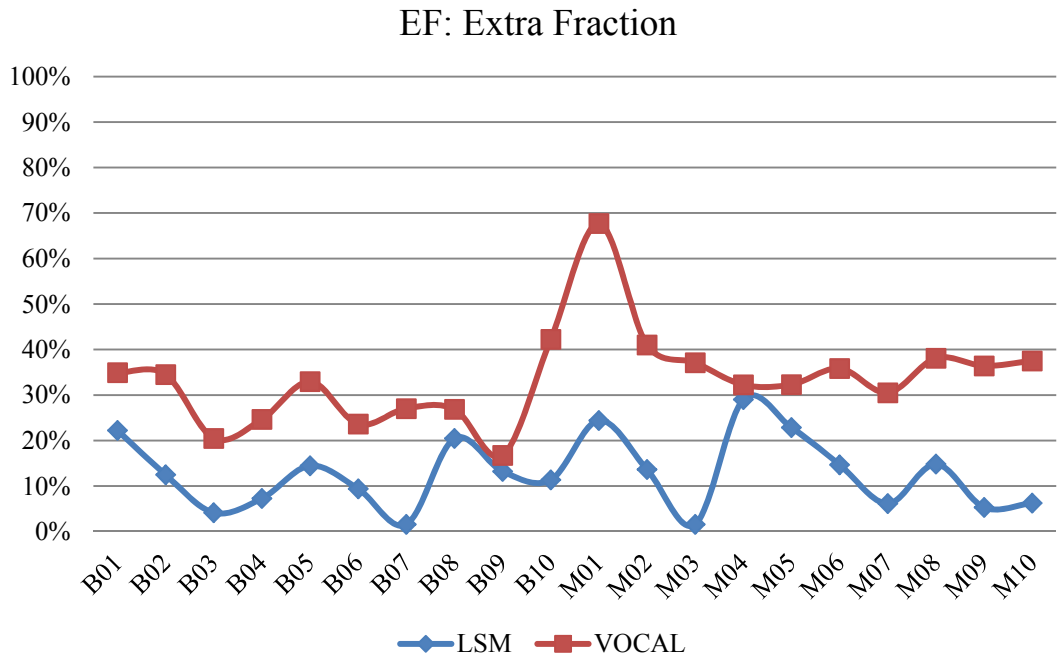

Figure 15. The extra fraction (EF) evaluation results of the assessment of our proposed LSM method and the VOCAL method

Table 3. The contouring evaluations using similarity index (SI) between our proposed LSM method and the VOCAL method

Pathology proven result	Average similarity index (SI)	
	The proposed LSM method	VOCAL mode
Benign case (10 cases)	**84.67%**	**80.81%**
Malignant case (10 cases)	**85.66%**	**81.91%**
All database (20 cases)	**85.17%**	**81.36%**

Table 4. The contouring evaluations using overlap fraction (OF) between our proposed LSM method and the VOCAL method

Pathology proven result	Average overlap fraction (OF)	
	The proposed LSM method	VOCAL mode
Benign case (10 cases)	**82.40%**	**87.66%**
Malignant case (10 cases)	**85.79%**	**96.08%**
All database (20 cases)	**84.09%**	**91.87%**

Table 5. The contouring evaluations using overlap value (OV) between our proposed LSM method and the VOCAL method

Pathology proven result	Average overlap value (OV)	
	The proposed LSM method	VOCAL mode
Benign case (10 cases)	**73.75%**	**68.36%**
Malignant case (10 cases)	**75.34%**	**69.47%**
All database (20 cases)	**74.54%**	**68.91%**

Table 6. The contouring evaluations using extra fraction (EF) between our proposed LSM method and the VOCAL method

Pathology proven result	Average extra fraction (EF)	
	The proposed LSM method	VOCAL mode
Benign case (10 cases)	**11.65%**	**28.41%**
Malignant case (10 cases)	**13.88%**	**38.88%**
All database (20 cases)	**12.76%**	**33.64%**

CHAPTER4

CONCLUSION

Today, in many diagnostic modalities of breast cancer, advantages of ultrasound are images-cost, easy to operate, non-radioactive, immediate angiography and non-invasive. Physicians generally utilized ultrasound images in tumor diagnosis and testing, moreover clinicians take it to test tumor biopsies to determine tumor benign and malignant. If a computer-aided system was useful to correct depiction of tumor contour, it would be help on improving physician diagnosis of benign and malignant tumors of the correct rate.

This study proposed a fast and high accuracy automatic 3D breast tumor image segmentation method. The proposed method performed the region growing produce to obtain the initial outline and get the final contouring results by using level-set method. This work kept away from the problem of level-set algorithm which needs a large amount of computation in 3D space, as well as resolved its problem of excessive dependence of initial contour in image segmentation.

According to the experimental 10 benign cases and 10 malignant cases showed that the methods used in this study can effectively cutting ultrasound imaging of tumor contours, its average value of SI can reach more than 85%; compared to the

VOCAL method of the EF average 34%, the proposed method can significantly reduce the value of the EF to 12%. For tumor contour cutting error has significantly improved. In our study, each case computing time required is approximately 120 seconds. Compared to other method of cutting, usually need several tens of minutes. Our proposed method has significant advantages, and for medical diagnostic applications have more practical assistance.

The proposed method was fully automated 3D breast tumor contour cutting. User only needed to select a region growing seed point, you will get breast cancer 3D contour cutting. Compared VOCAL method requires manual depicting six ultrasound images of the difference of 30 tumor contours, and physicians need to manually describe each one tumor contour method of rapid and convenient, which would help doctors in the diagnosis of convenience.

Due to the reduced time required for the program operation, the proposed method does not carry out pre-processing for the image, which causes the accuracy rate resulting of breast tumors contour will be decreased. Therefore, the future will face in combination with other effective filter to reduce noise, without increasing too much computation time of the situation and effectively enhance tumor contour cutting accuracy.

REFERENCES

[1] ACS, "Breast Cancer Facts and Figures 2009-2013.," American Cancer Society, 2013.

[2] C.M. Chen, Y.H. Chou, K.C. Han, G.S. Hung, C.M. Tiu, H.J. Chiou et al.,"Breast lesions on sonograms: computer-aided diagnosis with nearlysetting-independent features and artificial neural networks," Radiology, vol.226, no. 2, pp. 504-514, Feb. 2003.

[3] T. Chen and D. Metaxas, "A hybrid framework for 3D medical image segmentation," Med. Image Anal., vol. 9, no. 6, pp. 547-565, Dec. 2005.

[4] K. Horsch, M.L. Giger, L.A. Venta, and C.J. Vyborny, "Automatic segmentation of breast lesions on ultrasound," Med. Phys., vol. 28, no. 8, pp. 1652-1659, Aug. 2001.

[5] R.F. Chang, W.J. Wu, C.C. Tseng, D.R. Chen, and W.K. Moon, "3-D snake for US in margin evaluation for malignant breast tumor excision using Mammotome," IEEE Trans. Inf. Technol. Biomed., vol. 7, no. 3, pp. 197-201, Sept. 2003.

[6] A. Madabhushi and D.N. Metaxas, "Combining low-, high-level and empirical domain knowledge for automated segmentation of ultrasonic breast lesions," IEEE Trans. Med. Imaging, vol. 22, no. 2, pp. 155-169, Feb. 2003.

[7] Y. L. Huang, D. R. Chen and S. C. Chang, "Three-dimensional region-based segmentation for breast tumor on sonography", Journal of Ultrasound in Medicine, accepted, 2012.

[8] Linda G. Shapiro and George C. Stockman (2001): “Computer Vision”, pp 279-325, New Jersey, Prentice-Hall, ISBN 0-13-030796-3

[9] K. Haris, S.N. Efstratiadis, and N. Maglaveras (1998) “Watershed-based image segmentation with fast region merging,” in Proceedings of the IEEE International Conference on Image Processing, vol. 3, pp. 338-342.

[10] L. Vincent and P. Soille (June 1991) “Watersheds in digital spaces: an efficient algorithm based on immersion simulations,” IEEE Trans. Pattern Anal. Machine Intell., vol. 13, no. 6, pp. 583–598.

[11] K. Haris and S.N. Efstratiadis (Dec. 1998) “Hybrid image segmentation using watersheds and fast region merging” IEEE Trans. Image Processing, vol. 7, no. 12, pp. 1684-1699.

[12] Y. L. Huang and D. R. Chen, "Watershed Segmentation for Breast Tumor in 2-D Sonography", Ultrasound in Medicine and Biology, vol. 30, no. 5, pp. 625-632, May 2004.

[13] W. C. Kao, C. K. Yu, W. H. Chen, C. P. Shen and Y. W. Hung, “Automatic Electrocardiogram Recognition by Wavelet Transform and Support Vector Machine,” 2005 CACS Automatic Control Conference, Taiwan, Nov., 2005.

[14] J. Z. Xiao and Li Xiao, “A Research of the Partition Clustering Algorithm,” International Symposium on Intelligence Information Processing and Trusted Computing , 2010.

[15] Kass, M., A. Witkin, D. Terzopoulos,“Snakes: Active contour models,” Int. J. Comput. Vis., vol. 1, pp. 321–331, 1987.

[16] Zouina Aktouf, Gilles Bertrand, Laurent Perroton"A three-dimensional holes closing algorithm", Pattern Recognition Letters, Vol. 23, No. 5. (March 2002), pp. 523-531.

[17] Rolf Adams and Leanne Bischof, "Seeded Region growing," IEEE Transactions on Image processing, vol. 16, pp. 641-647, June1994.

[18] Andrew Mehnert and Paul Jackway, "An improved seeded region growing algorithm," Pattern Recognition Letters, vol. 18, pp. 1065-1071, 1997.

[19] C. Revol-Muller, F. Peyrin, Y. Carrillon, and C. Odet, “Automated 3D region growing algorithm based on an assessment function,” Pattern Recognition Letters, vol. 23, no. 1-3, pp. 137-150, Jan.2002.

[20] D. CohenOr and A. Kaufman, “3D line voxelization and connectivity control,” IEEE Computer Graphics and Applications, vol. 17, no. 6, pp. 80-87, Nov.1997.

[21] L. Pothuaud, P. Porion, E. Lespessailles, C. L. Benhamou, and P. Levitz, "A new method for three-dimensional skeleton graph analysis of porous media: application to trabecular bone microarchitecture," Journal of Microscopy-Oxford, vol. 199, pp. 149-161, Aug.2000.

[22] S. Osher and J. Sethian, “Fronts propagating with curvature dependent speed: algorithms based on the Hamilton-Jacobi formulation,” Journal of Computational Physics, vol. 79, pp. 12~49, 1988.

[23] T. Chan and L. Vese, “Active contours without edges,” IEEE Trans. Image Processing, vol. 10, No. 2, pp. 266–277, 2001.

[24] Y. L. Huang, Y. R. Jiang, D. R. Chen, and W. K. Moon, “Level set contouring for breast tumor in sonography,” Journal of Digital Imaging, vol. 20, no. 3, pp. 238-247, Sept. 2007.

[25] V. Caselles, R. Kimmel, and G. Sapiro, “Geodesic active contours,” Intl. Journal of Computer Vision, vol. 22, no. 1, pp. 61-79, 1997.

[26] N. J. Raine-Fenning, J. S. Clewes, N. R. Kendall, A. K. Bunkheila, B. K. Campbell, and I. R. Johnson, "The interobserver reliability and validity of volume calculation from three-dimensional ultrasound datasets in the in vitro setting," Ultrasound in Obstetrics & Gynecology, vol. 21, no. 3, pp. 283-291, Mar.2003.

[27] N. Raine-Fenning, B. Campbell, J. Collier, M. Brincat, and I. Johnson, "The reproducibility of endometrial volume acquisition and measurement with the VOCAL-imaging program," Ultrasound in Obstetrics & Gynecology, vol. 19, no. 1, pp. 69-75, Jan.2002.

[28] A. Bordes, A. M. Bory, M. Benchaib, R. C. Rudigoz, and B. Salle, "Reproducibility of transvaginal three-dimensional endometrial volume measurements with virtual organ computer-aided analysis (VOCAL) during ovarian stimulation," Ultrasound in Obstetrics & Gynecology, vol. 19, no. 1, pp. 76-80, Jan.2002.

[29] P. Anbeek, K. L. Vincken, M. J. P. van Osch, R. H. C. Bisschops, and J. van der Grond, “Probabilistic segmentation of white lesions in MR imaging,” Neuroimage, vol. 21, no. 3, pp. 1037-1044, Mar. 2004.